

Vibronic Koster-Slater impurity: Exactly soluble model of deep levels in semiconductors

Václav Špička, Pavel Lipavský, and Bedřich Velický

Institute of Physics, Czechoslovak Academy of Sciences, Na Slovance 2, 18040 Praha 8, Czechoslovakia

(Received 29 May 1992)

The Koster-Slater model of a deep impurity, extended by a single phonon mode coupled to the electron only at the impurity site, can be solved exactly, i.e., not using an adiabatic or static approximation. Total (vibronic) eigenenergies and eigenfunctions are derived and compared with the adiabatic ansatz.

I. INTRODUCTION

A charge transfer from or to a deep level is accompanied by a lattice reconstruction in the impurity vicinity. An energy gain of this reconstruction is typically greater than the energy of an associated phonon, therefore this interaction is not tractable in a weak coupling limit.¹ Since the electron-phonon interaction potential is not a good *small* term, other choices have been tested in literature. One of the most studied *small* terms is a non-adiabatic term of the Hamiltonian; this choice, however, turned out to be very controversial.² Why? Let us introduce a single collective coordinate Q to measure the lattice reconstruction. Within the adiabatic expansion the lattice kinetic energy is neglected and this reduced Hamiltonian is diagonalized in an electron subspace, specified by Q as a parameter. Then the lattice kinetic energy is introduced and the lattice vibrational spectra is derived under the assumption that electrons remain unexcited (for each Q they are always in their lowest energy state). The part of the Hamiltonian which drives electrons out of lowest state is the *small* term. This scheme is successful only if the electronic lowest state changes smoothly with the parameter Q . Unfortunately, this is not the case for all values of Q . As $-Q$ exceeds a certain value $-Q_c$, the bound state at the impurity site changes into a resonant level embedded in the continuum of extended states. The crossover coordinate Q_c is an upper bound on the domain of the adiabatic ansatz. The reconstruction of the ground state may begin for much smaller values of $-Q < -Q_c$, however, and we have to ask which is the actual regime in which the adiabatic approximation is applicable.

In this paper we want to touch the question from a different angle. We introduce a model of the deep impurity which keeps all important features (continuum of crystal states, localized impurity state, single phonon mode, and strong electron-phonon interaction), but is soluble to the end without adiabatic or other questionable approximation. The key point making the model soluble is a restriction of the electron-local phonon interaction to a finite range around the impurity site. This is very different from the customary model Hamiltonian, in which the impurity bound state is coupled to the local mode as a rigid whole. We believe that there are physical reasons for which our model of spatially restricted interaction is more adequate for substitutional impurities in

weakly polar materials. In real space, the electron-lattice coupling is proportional to the square of the electron amplitude at a given site which is singularly large near the impurity.

A particularly lucid and at the same time analytically tractable model includes a linear electron-phonon coupling only at the impurity site. Our method to solve for its vibronic eigenstates combines the method of Koster and Slater for phononless deep impurities³ and the recursion method for tridiagonal matrices. A review of exactly solved electron-boson models in condensed matter and molecular physics by a generalized recursion method is provided by Cini and D'Andrea.⁴ Our model is not identical with any of the models listed by Cini and D'Andrea, except in the limit of a flat conduction band when our solution can be mapped by a unitary transformation on the solution of a two-level atom driven by an external laser field, derived by Swain.⁵

The content of this paper is as follows. In Sec. II we extend the simplest but successful Koster-Slater model of a deep impurity³ by adding a single phonon mode, which is linearly coupled to the electron at the impurity site. In Sec. III this "vibronic Koster-Slater model" is treated in the adiabatic approximation as used by Makram-Ebeid and Lannoo.⁶ In Sec. IV we derive a secular equation for exact eigenenergies and continued-fraction-type formulas for the eigenfunctions. In Sec. V we compare the exact eigenfunctions with the adiabatic approximation. Appendix A discusses the empirical meaning and possibilities of determining the parameters of the model. Appendix B is devoted to a method of termination of the infinite continued fraction for the vibronic eigenstate.

II. VIBRONIC KOSTER-SLATER IMPURITY MODEL

The model introduced and qualitatively discussed in the Introduction can now be formally defined as follows. Let us assume an impurity which (1) is neutral in the empty state, (2) forms a single bound state moderately deep below the conduction band edge, and (3) strongly affects equilibrium positions of neighbor atoms according to its occupation.

The effective Hamiltonian we use to model such an impurity includes the following: (1) a tight-binding single-electron Hamiltonian H^c of the host crystal,

$$H^c = \sum_{i,\beta,j,\gamma} |i,\beta\rangle h^c(i,\beta;j,\gamma) \langle j,\gamma|, \quad (2.1)$$

where i, j denote sites and β, γ label orbitals; (2) an impurity potential V ,

$$V = |0\rangle v \langle 0|, \quad (2.2)$$

where $|0\rangle \equiv |i=0, \beta=s\rangle$ is a single s orbital at the impurity site; (3) a phonon Hamiltonian H^p with a single local mode

$$H^i = |0\rangle h^i \langle 0| = \kappa |0\rangle \left\{ |0\rangle \sum_{n=0}^{\infty} \sqrt{n+1} (|n\rangle \langle n+1| + |n+1\rangle \langle n|) \right\}, \quad (2.4)$$

where the operator of the coordinate Q is expressed in terms of the harmonic-oscillator eigenstates. The model given by this Hamiltonian, $H^c + V + H^p + H^i$, we will call a vibronic Koster-Slater impurity.

This model is the root member of the whole family of increasingly more realistic models having (i) more bands, (ii) more locally coupled modes, (iii) wider range of nonzero electron-phonon coupling. While all these models are similar in their basic behavior, our simplest model is distinguished by being soluble in a formally closed way. Assuming basic structure of the model, the parameters of H^c are empirically known. The Koster-Slater potential V is fitted to reproduce the empty impurity level, ω is the optical phonon frequency, and the coupling strength κ is fitted to reproduce the occupied impurity level in the ground state. More details about fitting the model parameters are given in Appendix A.

III. ADIABATIC APPROXIMATION

To get familiar with the physics of the vibronic Koster-Slater model, we start by looking at its eigenstates within the customary adiabatic approximation.

A. Adiabatic approximation

The adiabatic approximation is naturally expressed in the coordinate representation of the phonon Hamiltonian (2.3),

$$H^p = \frac{\omega}{2} \left[-\frac{\partial^2}{\partial Q^2} + Q^2 - 1 \right]. \quad (3.1)$$

We use the dimensionless coordinate Q to avoid an unknown *mass* associated with the oscillator. The electron-phonon interaction Hamiltonian (2.4) then reads

$$H^i = |0\rangle Q \kappa \sqrt{2} \langle 0|. \quad (3.2)$$

Within the adiabatic approach one first eliminates H^p and evaluates electronic states parametrized by Q ,

$$(E_Q - H^c) |\phi_Q\rangle = |0\rangle (v + Q \kappa \sqrt{2}) \langle 0| \phi_Q\rangle. \quad (3.3)$$

Equation (3.3) corresponds to a simple Koster-Slater impurity with Q -parametrized impurity potential. The analog of the secular equation (A3) corresponding to (3.3)

$$H^p = \sum_{n=0}^{\infty} |n\rangle n \omega \langle n|, \quad (2.3)$$

where $(Q|n\rangle)$ is the eigenfunction of the harmonic oscillator [note different brackets for single-electron wave function $\{ \}$, free phonon wave function $()$, and the total wave function $\langle \rangle$]; (4) and a linear electron-phonon interaction potential H^i , restricted to the s orbital,

then yields the parametrized *eigenenergy* E_Q ,

$$\frac{1}{\langle 0|G^c(E_Q)|0\rangle} = v + Q \kappa \sqrt{2}. \quad (3.4)$$

For $Q < Q_c$,

$$Q_c = \frac{1}{\kappa \sqrt{2}} \left[\frac{1}{\langle 0|G^c(0)|0\rangle} - v \right]; \quad (3.5)$$

the Koster-Slater impurity has no bound state and the ground state $|\phi_Q\rangle$ is identical to the lowest energy extended state $|\phi_0\rangle$ of the conduction band. Thus the electronic energy equals zero, the energy at the band edge.

Within the adiabatic approach the vibronic wave function, i.e., the total wave function of the electron-lattice complex, is approximated as

$$\langle Q|\Psi_m^{\text{ad}}\rangle = \chi_m(Q) |\phi_Q\rangle. \quad (3.6)$$

Substituting (3.6) into the Schrödinger equation, $(E - H^c - H^p - V - H^i)|\psi\rangle = 0$, leads to the equation for the vibronic eigenenergies

$$\langle \phi_Q | E_m^{\text{ad}} - \frac{\omega}{2} \left[-\frac{\partial^2}{\partial Q^2} + Q^2 - 1 \right] - E_Q \theta(Q - Q_c) | \phi_Q \rangle \chi_m(Q) = 0. \quad (3.7)$$

Equation (3.7) includes a nonadiabatic term following

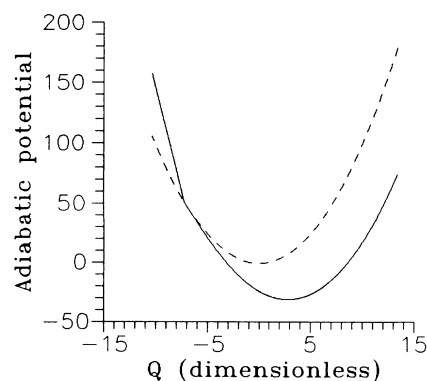


FIG. 1. Adiabatic and modified adiabatic potentials.

TABLE I. Table of exact and adiabatic eigenenergies. E_0 and E_0^{ad} are ground-state energies. The positive sign of E_{14}^{ad} shows that the 14th excited state is not bounded within the adiabatic approximation.

n	E_n	E_n^{ad}
0	-0.560 000 0	-0.534 740 7
1	-0.522 169 4	-0.495 450 5
2	-0.484 363 1	-0.456 160 8
3	-0.446 582 0	-0.416 870 8
4	-0.408 826 9	-0.377 580 9
5	-0.371 098 4	-0.338 291 0
6	-0.333 397 5	-0.299 001 0
7	-0.295 725 2	-0.259 711 1
8	-0.258 082 2	-0.220 421 2
9	-0.220 469 8	-0.181 131 2
10	-0.182 889 0	-0.141 841 3
11	-0.145 341 1	-0.102 551 4
12	-0.107 827 2	-0.063 261 5
13	-0.070 348 8	-0.023 971 6
14	-0.032 907 7	0.015 318 2

from the derivatives of $|\phi_Q\rangle$ with respect to Q . After this term is neglected the adiabatic equation for eigenenergies reads

$$\left[E_m^{\text{ad}} - \frac{\omega}{2} \left[-\frac{\partial^2}{\partial Q^2} + Q^2 - 1 \right] - E_Q \theta(Q - Q_c) \right] \chi_m(Q) = 0. \quad (3.8)$$

The nonadiabatic correction we do not discuss here. The adiabatic potential

$$\omega Q^2/2 + E_Q \theta \quad (3.9)$$

is in Fig. 1, the resulting eigenenergies are in Table I.

B. Modified adiabatic approximation

Strictly speaking, the adiabatic approximation applies only for single-electron states below the band edge which limits the allowed values of Q . We have in mind primarily the defects in direct zinc-blende semiconductors. In this case it is easy to include in a good approximation also deviations $Q < Q_c$ following the popular approach of Henry and Lang.⁷ Namely, the Γ minimum is accompanied by a weak density of states while the onset of the X and/or L minima comes at higher energies. This is reflected in our model by the assumed local density of states having a dominant shoulder at the high-energy region. Assuming the Γ part as a perturbation, we extend the adiabatic approach for resonant states simply ignoring the lowest energy extended state and keeping the resonant level E_Q for $Q < Q_c$ as an effective deformation potential. Thus we obtain a modified equation for eigenenergies

$$\left[\bar{E}_m^{\text{ad}} - \frac{\omega}{2} \left[-\frac{\partial^2}{\partial Q^2} + Q^2 - 1 \right] - E_Q \right] \tilde{\chi}_m(Q) = 0. \quad (3.10)$$

The extended effective deformation potential is shown in Fig. 1.

In fact, the detailed numeric study shows that for the vibronic Koster-Slater model and the parameters we use this approximation is fully equivalent to the adiabatic approximation, and we will not make an explicit distinction between the two approximations.

C. Matrix elements in the adiabatic approximation

The full vibronic state is a complex object. To gain its comprehensive characteristic, we look at its important matrix elements. As with the usual Koster-Slater impurity, the projection of the electron part on the central cell is crucial, only now we have to obtain it for each of the n -phonon components separately. We mention in passing that these elements alone determine, e.g., the ionization rates in an external electric field.

To evaluate the matrix elements $(n|\{0|\Psi_m^{\text{ad}}\})$ in the adiabatic approximation, we employ the coordinate representation

$$(n|\{0|\Psi_m^{\text{ad}}\}) = \int dQ (n|Q)(Q|\{0|\Psi_m^{\text{ad}}\}), \quad (3.11)$$

where

$$(n|Q) = \frac{1}{(\sqrt{\pi} 2^n n!)^{1/2}} H_n(Q) \exp[-Q^2/2] \quad (3.12)$$

is the eigenfunction of H^P . According to the adiabatic approximation (3.6) we get

$$(n|\{0|\Psi_m^{\text{ad}}\}) = \int dQ (n|Q) \{0|\phi_Q\} \chi_m(Q). \quad (3.13)$$

The amplitude of the electron wave function at the impurity site reads

$$\{0|\phi_Q\} = \left[\frac{\partial}{\partial E} \frac{1}{\{0|G^c(E)|0\}} \Big|_{E=E_Q} \right]^{-1/2} \theta(Q - Q_c). \quad (3.14)$$

The proof of (3.14) is identical to proof of (A16).

Within the adiabatic approximation the region $Q < Q_c$ does not contribute. In contrast, within the modified adiabatic approximation the integral is nontrivial in this region,

$$(n|\{0|\tilde{\Psi}_m^{\text{ad}}\}) = \int dQ (n|Q) \tilde{\chi}_m(Q) \times \left[\frac{\partial}{\partial E} \frac{1}{\{0|G^c(E)|0\}} \Big|_{E=E_Q} \right]^{-1/2}. \quad (3.15)$$

We note that $(n|\{0|\tilde{\Psi}_m^{\text{ad}}\})$ does not have a rigorous meaning of the wave function, since the electronic part is not well defined above the band edge.

We will discuss these adiabatic matrix elements in Sec. V together with their exact counterparts.

IV. EXACT EIGENSTATES OF THE VIBRONIC KOSTER-SLATER MODEL

In this section we find the bound eigenstates of the vibronic Koster-Slater model. In contrast to studies in print, we treat the Schrödinger equation directly, without

resorting to questionable approximations like adiabatic, static, and so on. The only approximations used are of the numerical kind necessary for an evaluation of closed explicit expressions; all of them are well under control.

A. Schrödinger equation

The stationary Schrödinger equation of the vibronic Koster-Slater model reads

$$(E_m - H^c - H^p)|\Psi_m\rangle = (V + H^i)|\Psi_m\rangle. \quad (4.1)$$

The vibronic wave function $|\Psi_m\rangle$ has both phonon and electronic variables.

With help of the free-particle resolvent

$$G^0(E) = \frac{1}{E - H^c - H^p} \quad (4.2)$$

we rearrange (4.1) as

$$|\Psi_m\rangle = G^0(E_m)(V + H^i)|\Psi_m\rangle. \quad (4.3)$$

Both the impurity potential V and the interaction Hamiltonian H^i affect only the orbital $|0\rangle$ at the impurity. Thus the vibronic wave function $|\Psi_m\rangle$ contributes to the right-hand side only by its elements at the impurity site, $\{0|\Psi_m\rangle$. Multiplying (4.3) by $\{0|$ one obtains a closed equation for these elements

$$(n|\{0|\Psi_m\rangle) = (n|\{0|G^0(E_m)|0\rangle)(v + h^i)\{0|\Psi_m\rangle}. \quad (4.4)$$

The free-particle resolvent can be remarkably simplified, because it is separable in the electron and the phonon variables. Within the diagonal representation of H^p , Eq. (2.3), the resolvent G^0 reads

$$G^0(E) = \sum_{n=0}^{\infty} |n\rangle G^c(E - n\omega)\langle n|, \quad (4.5)$$

where the host crystal single-electron resolvent G^c is given by

$$G^c(E) = \frac{1}{E - H^c}. \quad (4.6)$$

Putting (4.5) into (4.4) one finds

$$\frac{1}{\{0|G^c(E_m - n\omega)|0\rangle} \{0|(n|\Psi_m\rangle) = v\{0|(n|\Psi_m\rangle) + (n|h^i\{0|\Psi_m\rangle}. \quad (4.7)$$

This reduced Schrödinger equation will be the focus of our interest.

Equation (4.7) provides only the on-impurity elements of the wave function. To derive the off-impurity elements, one can combine (4.7) with (4.3). This provides an identity

$$(n|\{i,\beta|\Psi_m\rangle) = \{i,\beta|G^c(E_m - n\omega)|0\rangle \frac{1}{\{0|G^c(E_m - n\omega)|0\rangle} \{0|(n|\Psi_m\rangle). \quad (4.8)$$

The identity (4.8) is a very convenient tool for calculation of the wave function out of the impurity site. Once the values of the wave function are known at the impurity site, the total wave function results from the single-electron resolvent; note that the n -phonon component $(n|\{i,\beta|\Psi_m\rangle$ depends exclusively on the n -phonon component at the impurity site.

B. Recurrent relations and secular equation

Now we are ready to derive recurrent relations for the n -phonon components of the impurity-site element of the wave function. For the explicit h^i , Eq. (2.11), (4.7) goes into a three-term recurrence

$$\frac{1}{\{0|G^c(E_m - n\omega)|0\rangle} \{0|(n|\Psi_m\rangle) = v\{0|(n|\Psi_m\rangle) + \kappa\sqrt{n+1}\{0|(n+1|\Psi_m\rangle) + \kappa\sqrt{n}\{0|(n-1|\Psi_m\rangle). \quad (4.9)$$

We have to choose the boundary condition we will use while solving for $\{0|(n|\Psi_m\rangle$. One choice is to start from $\{0|(0|\Psi_m\rangle$ and for a trial E_m to monitor the asymptotics of $\{0|(n|\Psi_m\rangle$ for large n . If $\{0|(n|\Psi_m\rangle$ converges, E_m is an eigenenergy. An alternative approach starts from the asymptotics at large n and monitors whether the wave function reaches the correct ratio $\{1|(n|\Psi_m\rangle)/\{0|(n|\Psi_m\rangle$. The secular equation then follows from the condition for the 0-phonon element

$$\frac{1}{\{0|G^c(E_m)|0\rangle} \{0|(0|\Psi_m\rangle) = v\{0|(0|\Psi_m\rangle) + \kappa\{0|(1|\Psi_m\rangle). \quad (4.10)$$

In our discussion we use the second boundary condition

and the secular equation (4.10). In numerical implementations, however, we have used a combined method: starting simultaneously from $n=0$ and $n \rightarrow \infty$ we have monitored the matching at $n=m$. More details are below.

The recurrent relation (4.9) does not have constant coefficients, thus we have to solve it numerically. However, it is advantageous first to perform some algebraic rearrangements, which makes the recurrence more stable and efficient. In the case of constant coefficients, the solution has the form $\{0|(n|\Psi_m\rangle \sim \lambda^n$; in the case of nonconstant coefficients we express $\{0|(n|\Psi_m\rangle$ as

$$\{0|(n|\Psi_m\rangle) = \{0|(0|\Psi_m\rangle) \prod_{k=1}^n \lambda_k(E_m). \quad (4.11)$$

From (4.9) one finds that λ 's have to satisfy

$$\frac{1}{\{0|G^c(E_m - n\omega)|0\}} = v + \kappa\sqrt{n+1}\lambda_{n+1}(E_m) + \kappa\sqrt{n}\frac{1}{\lambda_n(E_m)}. \quad (4.12)$$

To simplify notation and to make a contact with the Green-function method, we introduce

$$\Gamma_n(E) = \frac{\lambda_n(E)}{\kappa\sqrt{n}}, \quad (4.13)$$

for which the recurrence reads

$$\frac{1}{\Gamma_n(E)} = \frac{1}{\{0|G^c(E - n\omega)|0\}} - v - \kappa^2(n+1)\Gamma_{n+1}(E). \quad (4.14)$$

According to our choice of the boundary condition, this recurrence should be solved in the descending direction, i.e., from $n = \infty$ stepping down to $n = 1$. The secular equation (4.10) in terms of Γ 's reads

$$\frac{1}{\{0|G^c(E)|0\}} = v + \kappa^2\Gamma_1(E). \quad (4.15)$$

It is advantageous to extend the range of Γ 's to $n=0$, defining Γ_0 from the recurrence (4.14) (λ_0 is undefined). The secular equation (4.15) then reads $\Gamma_0^{-1}(E)=0$.

To generate the solution $\{\Gamma_i\}$, we need the boundary condition for $n \rightarrow \infty$. This is provided in our case simply by

$$\lim_{n \rightarrow \infty} \Gamma_n \rightarrow 0. \quad (4.16)$$

To derive this limit, we have to start from the asymptotics of the resolvent

$$\{0|G^c(E - n\omega)|0\} \sim \frac{1}{n\omega}, \quad (4.17)$$

which for large n follows from (4.6). Assuming now $\Gamma_n \sim (n\omega)^\gamma$ we get

$$(n\omega)^{-\gamma} \sim n\omega - \frac{\kappa^2}{\omega}(n\omega)^{\gamma+1}. \quad (4.18)$$

The first right-hand-side term is dominant: the opposite assumption should mean $\gamma = -\frac{1}{2}$ which leads to contradiction. Thus we have more precisely

$$\Gamma_n \sim (n\omega)^{-1}. \quad (4.19)$$

In practice, we have—as always with continued fractions—to resort to some kind of termination at a large but finite N . The simplest and customary termination is

$$\Gamma_{N+1} = 0. \quad (4.20)$$

Varying N , we may find its values large enough for a saturation of this procedure. However, an improved formal termination may be generated using asymptotic expressions or its refinements. A physically appealing way of such termination whose convergence with increasing N is much faster than for (4.20) is described in Appendix B.

C. Eigenfunction normalization

Having Γ 's, the only missing component of the wave function is its norm, i.e., the element $\{0|(0|\Psi_m\rangle$. A straightforward numerical normalization would be inconvenient, because the wave function has two variables, phonon and electronic. Here we derive identities which make normalization easier.

According to (4.8) the norm of the eigenfunction is

$$1 \equiv \langle \Psi_m | \Psi_m \rangle = \sum_{n=0}^{\infty} |\{0|(n|\Psi_m\rangle|^2 \left[\frac{1}{\{0|G^c(E_m - n\omega)|0\}} \right]^2 \sum_{i,\beta} \{0|G^c(E_m - n\omega)|i,\beta\} \{i,\beta|G^c(E_m - n\omega)|0\}. \quad (4.21)$$

The sum over orbitals $|i,\beta\rangle$ represents the operator unity in the electron space,

$$1 = \sum_{n=0}^{\infty} |\{0|(n|\Psi_m\rangle|^2 \left[\frac{1}{\{0|G^c(E_m - n\omega)|0\}} \right]^2 \{0|G^c(E_m - n\omega)G^c(E_m - n\omega)|0\}. \quad (4.22)$$

According to (4.6) the product of two resolvents can be expressed in terms of the energy derivative

$$\{0|G^c(E - n\omega)G^c(E - n\omega)|0\} = -\frac{\partial}{\partial E} \{0|G^c(E - n\omega)|0\}. \quad (4.23)$$

Substituting (4.23) into (4.22) one finds

$$1 = \sum_{n=0}^{\infty} |\{0|(n|\Psi_m\rangle|^2 \frac{\partial}{\partial E} \frac{1}{\{0|G^c(E - n\omega)|0\}} \Big|_{E=E_m}. \quad (4.24)$$

The formula (4.24) is free of the integration over the electronic variable. We have used this formula in our numerical treatment.

D. Ward identity

The normalization condition can be transformed so that it will not contain an infinite sum. From (4.11) and (4.13) we express (4.24) in terms of Γ 's,

$$1 = |\{0|(0|\Psi_m)\rangle|^2 \sum_{n=0}^{\infty} \left[\prod_{k=1}^n \kappa^2 k \Gamma_k^2(E) \right] \frac{\partial}{\partial E} \frac{1}{\{0|G^c(E-n\omega)|0\}} \Big|_{E=E_m}. \quad (4.25)$$

The sum in (4.25) can be evaluated in a way similar to the geometric series. From (4.14) we express the derivative as

$$\frac{\partial}{\partial E} \frac{1}{\{0|G^c(E-n\omega)|0\}} = \frac{\partial}{\partial E} \frac{1}{\Gamma_n(E)} + \kappa^2(n+1) \frac{\partial}{\partial E} \Gamma_{n+1}(E). \quad (4.26)$$

Let us denote the product of the first term with its prefactor

$$A_n(E) = \left[\prod_{k=1}^n \kappa^2 k \Gamma_k^2(E) \right] \frac{\partial}{\partial E} \frac{1}{\Gamma_n(E)}. \quad (4.27)$$

The product of the second term with its prefactor reads

$$\left[\prod_{k=1}^n \kappa^2 k \Gamma_k^2(E) \right] \kappa^2(n+1) \frac{\partial}{\partial E} \Gamma_{n+1}(E) = - \left[\prod_{k=1}^{n+1} \kappa^2 k \Gamma_k^2(E) \right] \frac{\partial}{\partial E} \frac{1}{\Gamma_{n+1}(E)} = -A_{n+1}(E). \quad (4.28)$$

Now we substitute (4.26)–(4.28) into (4.25),

$$\begin{aligned} 1 &= |\{0|(0|\Psi_m)\rangle|^2 \sum_{n=0}^{\infty} [A_n(E_m) - A_{n+1}(E_m)] \\ &= |\{0|(0|\Psi_m)\rangle|^2 A_0(E_m). \end{aligned} \quad (4.29)$$

From (4.29) and (4.27) one obtains the final relation

$$|\{0|(0|\Psi_m)\rangle|^2 = \left[\frac{\partial}{\partial E} \frac{1}{\Gamma_0(E)} \right]^{-1} \Big|_{E=E_m}. \quad (4.30)$$

Equation (4.30) is not an accidental property of the model but a special case of the Ward identity.

E. Formal solution

Now we can write down an explicit expression for the vibronic eigenfunction. From (4.11), (4.13), and (4.30) we have the values of the impurity-site elements

$$\langle n|0|\Psi_m\rangle = \left[\frac{\partial}{\partial E} \frac{1}{\Gamma_0(E)} \right]^{-1/2} \prod_{k=1}^n \kappa \sqrt{k} \Gamma_k(E) \Big|_{E=E_m}. \quad (4.31)$$

Once the impurity-site elements are known, the complete eigenfunction is given by (4.8).

For the reader who prefers wave functions to resolvents we provide a more explicit derivation of the off-impurity elements. Substituting (4.7) into (4.1) one finds that the n -phonon component of the eigenfunction satisfies a free-electron-like equation

$$\begin{aligned} (E_m - n\omega - H^c)(n|\Psi_m\rangle \\ = |0\rangle \frac{1}{\{0|G^c(E_m - n\omega)|0\}} \{0|(n|\Psi_m)\rangle. \end{aligned} \quad (4.32)$$

Note that a single n occurs and that E_m is already known. We can introduce an effective potential

$$V^{\text{eff}}(E) = |0\rangle \frac{1}{\{0|G^c(E)|0\}} \{0|, \quad (4.33)$$

within which Eq. (4.32) reads

$$[E_m - n\omega - H^c - V^{\text{eff}}(E_m - n\omega)](n|\Psi_m\rangle = 0. \quad (4.34)$$

Solution of the free-electron-like equation (4.34) can be obtained by any standard procedure. In contrast to a genuine free-electron Schrödinger equation the wave function $(n|\Psi\rangle$ is not normalized to unity but its value at the impurity site is fixed by (4.31).

F. Numerical calculations of matrix elements

The ansatz (4.11) is convenient for an analytic discussion; however, it does not provide the best numerical recipe. This is clear in a weak interaction limit, $\kappa \rightarrow 0$, when $\{0|(n|\Psi_m)\rangle \rightarrow \delta_{nm} \{0|\phi\}$, see (A12). Therefore the element $\{0|(0|\Psi_m)\rangle$ goes to zero for $m \neq 0$, making the formula (4.11) numerically unstable. While we are not concerned with the weak interaction limit, this numerical instability appears anyway for high excitations which have the 0-phonon element rather small.

The modified ansatz we use for numerical treatment is

$$\begin{aligned} \{0|(n|\Psi_m)\rangle &= \{0|(m|\Psi_m)\rangle \quad \text{for } n = m \\ &= \{0|(m|\Psi_m)\rangle \prod_{k=m+1}^n \kappa \sqrt{k} \Gamma_k(E_m) \\ &\hspace{15em} \text{for } n > m \\ &= \{0|(m|\Psi_m)\rangle \prod_{k=m-1}^n \kappa \sqrt{k+1} \Delta_k(E_m) \\ &\hspace{15em} \text{for } n < m. \end{aligned} \quad (4.35)$$

Here, Γ 's are given by (4.13) and (4.14). Similarly, from the Schrödinger equation (4.9) one finds that Δ 's satisfy

$$\frac{1}{\Delta_n(E)} = \frac{1}{\{0|G^c(E-n\omega)|0\}} - v - \kappa^2 n \Delta_{n-1}(E). \quad (4.36)$$

The secular equation is obtained from the matching of the wave function at $n = m$,

$$\frac{1}{\{0|G^c(E-m\omega)|0\}} - v - \kappa^2 m \Delta_{m-1}(E) - \kappa^2(m+1)\Gamma_{m+1}(E) = 0. \quad (4.37)$$

For $\kappa \rightarrow 0$ this secular equation is as regular as the free electron secular equation.

Our numerical treatment is the following. In the region of expected eigenenergies we take energy as a parameter, evaluate Γ 's and Δ 's and then the left-hand side of (4.37). Since the left-hand side of (4.37) is a regular function of the energy E , we use Newton's iteration method in the vicinity of the eigenenergy. Then we evaluate $|\Psi_m\rangle$ from (4.35) and normalize according to (4.24).

V. COMPARISON OF EXACT AND ADIABATIC RESULTS

Comparing exact and adiabatic results one can ask two different questions: (1) How accurate is the adiabatic approximation for the given set of parameters? (2) Is it possible to adjust parameters for the adiabatic treatment so that the exact results are reproduced; and how much would the adjusted parameters differ from the original ones? From the first question we can learn about the reliability of the adiabatic treatment as applied to *ab initio* parameters, from the second one we can learn conversely about the reliability of deep impurity parameters obtained by an adiabatic fit to experimental data.

In Table I we compare the eigenenergies. The adiabatic eigenenergies are crudely by $\omega/2$ too high, and they are well equidistant with an energy difference comparable to the exact results. As a consequence, the number of bound adiabatic eigenstates is smaller than the number of the exact states. The right ground-state energy can be adjusted by taking a more attractive Koster-Slater potential or by increasing the amplitude of the electron-phonon interaction, but this straightforward parameter adjustment leads to a worse agreement of the wave functions.

Three of the wave functions are compared in Fig. 2. The ground state ($m=0$) provides a quite satisfactory agreement, assuming that high elements are irrelevant for the experiment. In the moderately excited state ($m=4$) we observe that the adiabatic wave has a correct range of amplitudes, but these amplitudes are systematically shifted towards larger n . Because of the discrete character of the quantum number n , the adiabatic approximation seems to provide rather poor values in the region of small n (< 5). This ill behavior in the small- n region is fully appreciable for the highly excited state ($m=8$). However, the order of magnitude is still comparable provided that we do not compare them for individual n but rather in some overall picture.

The adiabatic wave function can be adjusted to the exact one with a surprising accuracy; see Fig. 2. Since the share of the large- n components increases with the electron-phonon interaction, one can squeeze the adiabatic wave functions closer to the exact ones taking a *weaker* interaction strength. Note that with the weaker interaction the ground state floats even higher, in contrast to what we need to adjust the eigenenergies. At the same

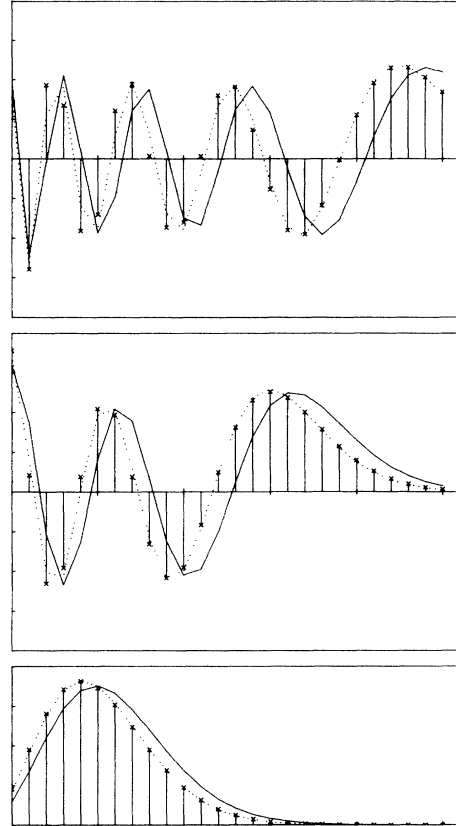


FIG. 2. Exact, adiabatic and fitted adiabatic wave functions. Elements $\{0|(n|\Psi_m\rangle\}$ of the exact (needles), $\{0|(n|\Psi_m^{\text{ad}}\rangle\}$ adiabatic (full line), and $\{0|(n|\Psi_m^{\text{fit}}\rangle\}$ (dotted line) are plotted for $m=8$ (a), $m=4$ (b), and $m=0$ (c). n is on horizontal axis. Shift to high values of n in the adiabatic case and a good agreement in the fitted adiabatic case are apparent.

time the energy difference is getting closer to ω , again an undesirable side effect of the fitting. To compensate for these side effects it is inevitable to take an even more attractive Koster-Slater potential and to change also the free-phonon energy. The effective parameters corresponding to the fitted adiabatic wave functions in Fig. 2 are: $\kappa^{\text{fit}} = -0.106$ eV while $\kappa = -0.119$ eV, $\omega^{\text{fit}} = 0.0384$ eV while $\omega = 0.04$ eV, and $v^{\text{fit}} = -6.5$ eV while $v = -6.42$ eV. We note that the Koster-Slater potential v is referred to the band center, therefore one has to subtract the band half-width W ($=6$ eV) to judge the relative change. This change of the Koster-Slater potential causes a shift of the empty impurity energy level, $E_a^{\text{fit}} = -0.45$ eV while $E_a = -0.4$ eV. Briefly, for the vibronic Koster-Slater impurity with the above parameters, the adiabatic approximation leads to about 10% deviations, which is not that bad assuming an uncertainty one meets when looking for deep level parameters.⁸

VI. CONCLUSIONS

When asking what is the essential message of this work, we may single out three points.

- (i) An exactly soluble vibronic model of a deep level

impurity can be constructed so that it closely follows some real defects in semiconductors.

(ii) Testing the adiabatic approximation for reasonable defect parameters which are "intermediate," i.e., definitely out of the true adiabatic limit, we find a quantitative discrepancy both for the eigenenergies and eigenfunctions. To a high accuracy, it can be compensated for by adjusting all the parameter values by about 10%. This somewhat unexpected result would be important for judging the quality of empirically derived parameters of defects; further confirmation is certainly needed.

(iii) From a more basic point of view, this result suggests that the *structure* of the adiabatic wave functions is rather close to the reality: a suitable renormalization makes the adiabatic ansatz valid far outside its nominal domain of validity.

The proposed model allows for some generalizations: (1) one can assume more impurity states, all affected by electron-phonon interaction; (2) long-range impurity potential can be taken into account provided that the electron-phonon interaction remains localized; (3) electron-phonon interaction can be extended to tight-binding hopping elements to the impurity site; (4) the nonharmonic free phonon Hamiltonian is tractable; (5) nonlinear electron-phonon interaction is allowed. Any of these generalizations would just cost an additional numerical effort, while the basic structure of the solutions would be preserved.

ACKNOWLEDGMENTS

We are grateful to Jan Mašek for stimulating discussions and ideas.

APPENDIX A: PARAMETERS OF THE HAMILTONIAN

In this appendix we derive the magnitude of the Koster-Slater potential v and of the interaction constant κ , using a host crystal local density of states $h(E)$, an energy level E_u ($= -0.4$ eV) of the unoccupied impurity, and the ground-state energy E_g ($= -0.56$ eV) of the occupied impurity. While parameters used in this paper are rather *typical values* than real values corresponding to a specific impurity, we want to relate them to quantities that may be obtained from independent experiments, i.e., other than the deep level transient spectroscopy. Thus we assume that the local density of states follows from the electronic band structure, the energies E_u and E_g can be deduced from optical measurement. The remaining parameter is the phonon frequency ω , which we take equal to the optical phonon frequency ($= 0.04$ eV), although another value might be reasonable in the presence of a local vibrational mode. Clearly, we do not fit the parameters to deep level emission rates, which we will study using this model in the next paper.

1. Koster-Slater potential v

The energy level E_u of the unoccupied impurity does not depend on the phonon part of the Hamiltonian. Thus it is an eigenenergy of the electronic part $H^c + V$. We use this property to fit v from the free-electron Schrödinger equation

$$(E_u - H^c)|\phi\rangle = V|\phi\rangle. \quad (\text{A1})$$

Using (2.2),

$$|\phi\rangle = \frac{1}{E_u - H^c} V|\phi\rangle = G^c(E_u)|0\rangle v|0\rangle, \quad (\text{A2})$$

where we *define* the crystal resolvent G^c . From (A2) we get the Koster-Slater potential v in terms of the resolvent

$$v = \frac{1}{\langle 0|G^c(E_u)|0\rangle}. \quad (\text{A3})$$

2. Local resolvent $G^c(E)$

Now we need an explicit local resolvent $\langle 0|G^c(z)|0\rangle$. To construct this function we assume that we know a density of states $h(E)$ at the impurity site. These two functions are real and imaginary parts of a single analytic function (retarded Green function), therefore they are connected via the Hilbert transformation

$$\langle 0|G^c(E)|0\rangle = - \int \frac{d\mu}{\pi} \frac{h(\mu)}{\mu - E}. \quad (\text{A4})$$

In our calculations we have used a model $h(E)$, the Hubbard bubble skewed by Chebyshev polynomials,

$$h(E) = \frac{2}{W} (1 - z^2)^{1/2} (1 + b_1 z + b_3 z^3) \Big|_{z=E/W-1}. \quad (\text{A5})$$

Its parameters are chosen to reproduce a conduction band width $2W$ ($= 12$ eV) and the effective electron mass m (0.2 of the electron mass in the vacuum) at the band edge. The parameter b_3 results from the fit of the band edge to the parabolic electron band,

$$b_3 = -\frac{1}{2} + \frac{1}{16\pi} \left[\frac{a\sqrt{mW}}{\hbar} \right]^3, \quad (\text{A6})$$

where a ($= 0.55 \times 10^{-9}$ m) is a lattice constant. The parameter b_1 defines the extent of the paraboliclike region in the vicinity of the band edge; we use $b_1 = -3b_3$. We note that the total density of states is normalized to unity (the integral over energy equals π).

This model provides an explicit analytic formula for the resolvent

$$\langle 0|G^c(E)|0\rangle = \frac{2}{W} \left[z + b_3 z^4 + \left[b_1 - \frac{b_3}{2} \right] z^2 - \left[\frac{b_1}{2} + \frac{b_3}{8} \right] \right] + \theta(z^2 - 1) \frac{2}{W} (z^2 - 1)^{1/2} (1 + b_1 + b_3 z^3) \Big|_{z=E/W-1}. \quad (\text{A7})$$

3. Interaction constant κ

The exact value of κ , which reproduces the energy of the ground state, can be obtained only by trial and error, solving the secular equation for different values of κ . To get an estimator for the starting value of κ a linear approximation of the reciprocal resolvent can be used:

$$\frac{1}{\{0|G^c(E)|0\}} - v \approx (E - E_u) \frac{\partial}{\partial E} \frac{1}{\{0|G^c(E)|0\}} \Big|_{E=E_u}. \quad (\text{A8})$$

Equation (4.7) then becomes

$$(E - H^p - E_u) \frac{\partial}{\partial E} \frac{1}{\{0|G^c(E)|0\}} \Big|_{E=E_u} \{0|\Psi\} = \{0|H^i|\Psi\}. \quad (\text{A9})$$

Equation (A9) is equivalent to the Schrödinger equation of the harmonic oscillator with a shifted coordinate origin. This can be seen from a rearrangement

$$(E - E_u - H^p - H_{\text{eff}}^i) \{0|\Psi\} = 0, \quad (\text{A10})$$

where the effective interaction Hamiltonian is identical with H^i , except for the reduced interaction constant κ ,

$$\kappa_{\text{eff}} = \kappa \left[\frac{\partial}{\partial E} \frac{1}{\{0|G^c(E)|0\}} \Big|_{E=E_u} \right]^{-1}. \quad (\text{A11})$$

The shift of the ground-state energy of the effective Hamiltonian $H^p + H_{\text{eff}}^i$, related to the ground state of H^p , is known to be $\Delta E = -\kappa_{\text{eff}}^2/\omega$. This shift is equal to the difference between the ground-state energy and the empty impurity level, $\Delta E = E_g - E_u$. Therefore the interaction constant κ reads

$$\kappa = -\sqrt{(E_u - E_g)\omega} \frac{\partial}{\partial E} \frac{1}{\{0|G^c(E)|0\}} \Big|_{E=E_u}. \quad (\text{A12})$$

For our parameters the formula (A12) provides $\kappa = -0.129$ eV; the correct value is -0.119 eV.

The reduction of the interaction constant expressed by (A11) follows from the overlap of the interaction Hamiltonian with the bound-state wave function. In a weak coupling limit the electronic part of the wave function is crudely equal to the free-electron bound state $|\phi\rangle$. Thus one expects the reduction of the interaction constant in a form

$$\kappa_{\text{eff}} = \kappa |\{0|\phi\}|^2. \quad (\text{A13})$$

One can prove that (A11) is identical to (A13) using again the Ward identity. The norm of $|\phi\rangle$ evaluated from (A2) with v given by (A3),

$$\begin{aligned} 1 &\equiv \{\phi|\phi\} \\ &= |\{0|\phi\}|^2 \left[\frac{1}{\{0|G^c(E_u)|0\}} \right]^2 \{0|G^c(E_u)G^c(E_u)|0\}, \end{aligned} \quad (\text{A14})$$

then provides

$$|\{0|\phi\}|^2 = \left[\frac{\partial}{\partial E} \frac{1}{\{0|G^c(E)|0\}} \Big|_{E=E_u} \right]^{-1}, \quad (\text{A15})$$

which proves the relation between (A13) and (A11).

APPENDIX B: TERMINATION OF THE RECURRENCE

In this appendix we derive an approximative formula for $\Gamma_n(E)$ that can be used to start the descending recurrence (4.14). To this end we reverse the procedure used in the main text and utilize the Schrödinger equation (4.7) to discuss the asymptotics of the wave function. The starting value of Γ will be deduced from this asymptotics.

In Sec. IV we use the simplest termination $\Gamma_{N+1} = 0$. Within the Schrödinger equation (4.7) such termination corresponds to taking $\{0|(n|\Psi)\} = 0$ for $n > N$. Such a solution can be obtained sending $1/\{0|G^c(E_m - n\omega)|0\} \rightarrow \infty$ for $n > N$. This indirect way of cutoff has an advantage in that it can be done for the wave functions and Γ 's in a consistent manner.

Instead of the abrupt infinite ‘‘barrier’’ one can use some tractable approximation of $1/\{0|G^c(E_m - n\omega)|0\}$ for $n > N$. As is shown in Sec. IV, in the limit $n \rightarrow \infty$, the elements $\kappa\sqrt{n}\Gamma_n$ go to zero, therefore $\{0|(n|\Psi_n)\}$ decays to zero even faster than an exponential. Thus, for large N only a few elements $\{0|(n|\Psi_n)\}$ with $n > N$ give an appreciable contribution and we can focus on the vicinity of N . Therefore, for $E < E_{\text{cut}}$ ($E_{\text{cut}} \approx E_0 - N\omega$) we approximate the local resolvent $1/\{0|G^c(E)|0\}$ by its linear extrapolation from E_{cut} .

The linear approximation of the asymptotic region has a well-defined asymptotic behavior. Indeed, for $N \rightarrow \infty$, $1/\{0|G^c(E_m - N\omega)|0\} \rightarrow -N\omega$, thus the linear approximation is exact in this limit. At the same time, the superexponential decay of the wave function shrinks the width of the significant vicinity of N . For parameters used in our model this second reason of convergence is the dominant one.

1. Auxiliary eigenstates

According to the recursion (4.14), $\Gamma_{N+1}(E)$ depends only on $\{0|G^c(E')|0\}$ for $E' < E - N\omega$. Therefore, to evaluate $\Gamma_{N+1}(E)$ we can replace $1/\{0|G^c(E)|0\}$ by a linear function of E for all energies,

$$\frac{1}{\Gamma_n(E)} = \frac{1}{\{0|G^c(E_{\text{cut}})|0\}} - v \frac{\partial}{\partial E} \frac{1}{\{0|G^c(E)|0\}} \Big|_{E_{\text{cut}}} (E - n\omega - E_{\text{cut}}) - \kappa^2(n+1)\Gamma_{n+1}(E), \quad (\text{B1})$$

$$\frac{1}{\Gamma_n(E)} = \frac{E - n\omega - A}{B} - \kappa^2(n+1)\Gamma_{n+1}(E). \quad (\text{B1}')$$

Here (B1') introduces a reduced notation. Within this approximation, the share of the single-electron wave function at the central cell does not depend on the energy E (see Appendix A), thus the electronic part of the wave function is effectively decoupled.

While the recurrence (B1) is of the same complexity as (4.14), Eq. (4.7) can be, for $1/\{0|G^c(E)|0\}$ linear, solved directly:

$$(E - n\omega - A)\{0|(n|\tilde{\Psi}_m)\} = B(n|h^i\{0|\tilde{\Psi}_m)\}. \quad (\text{B2})$$

We use the tilde to distinguish the auxiliary wave functions. Indeed, we can separate the kinetic and potential parts of H^p in Eq. (B2), which allows us to express (B2) within Q representation, see (3.1) and (3.2),

$$(E - A)\{0|(Q|\tilde{\Psi}_m)\} + \frac{\omega}{2} \left[-\frac{\partial^2}{\partial Q^2} + Q^2 - 1 \right] \{0|(Q|\tilde{\Psi}_m)\} = QB\kappa\sqrt{2}\{0|(Q|\tilde{\Psi}_m)\}. \quad (\text{B3})$$

Now we merge the quadratic potential with the linear interaction potential into a new quadratic potential with a shifted bottom,

$$\left[E - A - \frac{Q_s^2\omega}{2} \right] \{0|(Q|\tilde{\Psi}_m)\} + \frac{\omega}{2} \left[-\frac{\partial^2}{\partial Q^2} + (Q - Q_s)^2 - 1 \right] \{0|(Q|\tilde{\Psi}_m)\} = 0, \quad (\text{B4})$$

where

$$Q_s = \frac{B\kappa}{\sqrt{2}}. \quad (\text{B5})$$

Except for a prefactor, the auxiliary wave functions $\{0|(Q|\tilde{\Psi}_m)\}$ are eigenfunctions of shifted harmonic oscillator

$$\{0|(Q|\tilde{\Psi}_m)\} = \left[\frac{B}{\sqrt{\pi m! 2^m}} \right]^{1/2} H_m(Q - Q_s) e^{-(Q - Q_s)^2/2}. \quad (\text{B6})$$

The auxiliary eigenenergy is

$$\bar{E}_m = A - \frac{Q_s^2\omega}{2} + m\omega. \quad (\text{B7})$$

2. Asymptotic Γ 's

At eigenenergies one can reverse the procedure used in the paper and evaluate Γ 's from wave functions. Accord-

ing to (4.31) a reversed relation reads

$$\Gamma_n(E^m) = \frac{1}{\kappa\sqrt{n}} \frac{\{0|(n|\Psi^m)\}}{\{0|(n-1|\Psi^m)\}}. \quad (\text{B8})$$

As mentioned above, $\Gamma_{N+1}(E)$ is independent from $1/\{0|G^c(E)|0\}$ for $E > E_{\text{cut}}$. Therefore Γ_{N+1} resulting from the auxiliary function (i.e., with linearized $1/\{0|G^c(E)|0\}$ on the whole E axis) is identical to Γ_{N+1} obtained for linearization restricted to the asymptotic region. The only limitation is that the auxiliary eigenenergies are different from their exact counterparts, therefore we have to interpolate to obtain a desired value.

3. Nested products

For convenience we include some algebra that makes the numerical implementation effective. The auxiliary wave function in the representation of free-phonon eigenstates reads

$$\{0|(n|\tilde{\Psi}_m)\} = \int dQ \frac{1}{(\sqrt{\pi n! 2^n})^{1/2}} H_n(Q) e^{-Q^2/2} \frac{\sqrt{B}}{(\sqrt{\pi m! 2^m})^{1/2}} H_m(Q - Q_s) e^{-(Q - Q_s)^2/2} \quad (\text{B9})$$

$$= \frac{\sqrt{B} Q_s^{n+m} e^{-Q_s^2/4}}{\sqrt{n! m! 2^{n+m}}} \sum_{p=0}^m \frac{n! m! (-1)^m}{(n-p)! (m-p)! p!} \left[\frac{2}{Q_s^2} \right]^p. \quad (\text{B10})$$

The wave function rapidly decays for large n , but the ratio of two neighbor elements allows for analytic cancellation that removes possible numerical difficulties. Using (B10) in (B8) one finds

$$\Gamma_{N+1}(\bar{E}_m) = \frac{Q_s \sqrt{B}}{\kappa(N+1)\sqrt{2}} \frac{C(N+1, m, 2Q_s^{-2})}{C(N, m, 2Q_s^{-2})}, \quad (\text{B11})$$

where

$$C(N, m, x) = \sum_{p=0}^N \frac{N! m!}{(N-p)! (m-p)! p!} x^p. \quad (\text{B12})$$

The function C can be expressed with help of nested products

$$C(N, m, x) = \left[1 + \frac{Nm}{1} x \left[1 + \cdots \left[1 + \frac{(N-m+2)2}{m-1} x \left[1 + \frac{(N-m+1)1}{m} x \right] \right] \cdots \right] \right], \quad (\text{B13})$$

which makes the application fast and numerically stable.

Let us summarize. Equation (B11) supported by the nested products (B13) provides values of Γ_{N+1} for energies equal to auxiliary eigenenergies $\{\tilde{E}_m\}$. The desirable value is obtained by the interpolation. We note that the procedure works well if the cutoff point is in the region where the eigenfunction is in the asymptotic exponential tail. For our model one can take N as low as 35 without a significant influence on the resulting eigenstates.

¹M. Lannoo and J. Bourgoin, *Point Defects in Semiconductors I; Theoretical Aspects*, Springer Series in Solid State Sciences, Vol. 22 (Springer, Berlin, 1981); M. Lannoo and J. Bourgoin, *Point Defects in Semiconductors II; Experimental Aspects*, Springer Series in Solid State Sciences Vol. 35 (Springer, Berlin, 1983).

²M. Wagner, *Phys. Status Solidi B* **115**, 427 (1983).

³G. F. Koster, and J. C. Slater, *Phys. Rev.* **95**, 1167 (1954); **96**, 1208 (1954).

⁴M. Cini and A. D'Andrea, *J. Phys. C: Solid State Phys.* **21**, 193 (1988).

⁵S. Swain, *J. Phys. A: Math., Nucl. Gen.* **6**, 1919 (1973).

⁶S. Makram-Ebeid and M. Lannoo, *Phys. Rev. B* **25**, 6406 (1982).

⁷C. H. Henry and D. V. Lang, *Phys. Rev. B* **15**, 989 (1977).

⁸F. Bridges, G. Davies, J. Robertson, and A. M. Stoneham, *J. Phys.: Condens Matter* **2**, 2875 (1990).